

## New transformation mechanism for a zinc-blende to rocksalt phase transformation in MgS

This article has been downloaded from IOPscience. Please scroll down to see the full text article.

2009 J. Phys.: Condens. Matter 21 452204

(<http://iopscience.iop.org/0953-8984/21/45/452204>)

View [the table of contents for this issue](#), or go to the [journal homepage](#) for more

Download details:

IP Address: 129.252.86.83

The article was downloaded on 30/05/2010 at 06:01

Please note that [terms and conditions apply](#).

## FAST TRACK COMMUNICATION

# New transformation mechanism for a zinc-blende to rocksalt phase transformation in MgS

**Murat Durandurdu**

Department of Physics, University of Texas at El Paso, El Paso, TX 79968, USA

and

Fizik Bölümü, Ahi Evran Üniversitesi, Kırşehir 40100, Turkey

Received 7 September 2009, in final form 2 October 2009

Published 21 October 2009

Online at [stacks.iop.org/JPhysCM/21/452204](http://stacks.iop.org/JPhysCM/21/452204)**Abstract**

The stability of the zinc-blende structured MgS is studied using a constant pressure *ab initio* molecular dynamics technique. A phase transition into a rocksalt structure is observed through the simulation. The zinc-blende to rocksalt phase transformation proceeds via two rhombohedral intermediate phases within  $R3m$  (No:160) and  $R\bar{3}m$  (No:166) symmetries and does not involve any bond breaking. This mechanism is different from the previously observed mechanism in molecular dynamics simulations.

(Some figures in this article are in colour only in the electronic version)

The pressure-induced phase transformations from the fourfold to sixfold coordinated structure in binary semiconducting compounds are a fundamental topic in condensed matter physics. Of particular interest are zinc-blende (ZB) type materials. The ZB to rocksalt (RS) phase transition has been studied extensively for decades and considerable information concerning this phase change has been obtained. Yet a clear atomic level picture of this phase transition could not be obtained in static high pressure experiments. In the past few years, much effort has been devoted to determine the transition mechanism of the ZB-to-RS phase transition because an understanding of its mechanism is very important for technological applications and controlling transition processes.

Because of the limitations of experimental information at the atomistic level, reliable dynamical simulations are desirable. Such simulations may fully describe the microscopic nature of transformation mechanisms and the electronic structure of phases for each applied pressure. Recent molecular dynamics (MD) simulation using an inter-atomic potential [1] revealed that the ZB-to-RS transformation of SiC is due to a cubic to monoclinic unit cell transformation such that Si and C sublattices shift with respect to each other along the [100] direction in the ZB structure. Furthermore, the transformation proceeds continuously without any bond

breaking, in contrast to the transformation mechanism based on a rhombohedral  $R3m$  intermediate state proposed in a first-principles calculation [2]. Motivated by the MD simulation [1], Catti [3] proposed an orthorhombic intermediate state with a  $Pmm2$  symmetry, having a much lower activation energy than  $R3m$ . The space group of this intermediate state later was corrected to  $Imm2$  because  $Imm2$  is actually one of the maximal subgroups of the ZB structure [4]. Recent *ab initio* simulations [5] show that this orthorhombic intermediate state is a universal transition state for the ZB-to-RS transition in semiconductor compounds, indicating that the transition state is independent of their ionicity.

The ZB-to-RS phase change is a reconstructive phase transformation and involves large atomic displacements. Therefore, the system can transform from one phase to another by passing through various closely related paths during the transition [6]. In other words, the transformation mechanism might follow various transition pathways or involve several intermediate states. Indeed, recent systematic group-theoretical analysis proposed several competitive low barrier pathways for the ZB-to-RS transformation of SiC in addition to the  $Imm2$  phase [7]. In our earlier work, using a constant pressure *ab initio* technique, we showed that the ZB-to-RS phase change of SiC, ZnSe and ZnS is based on

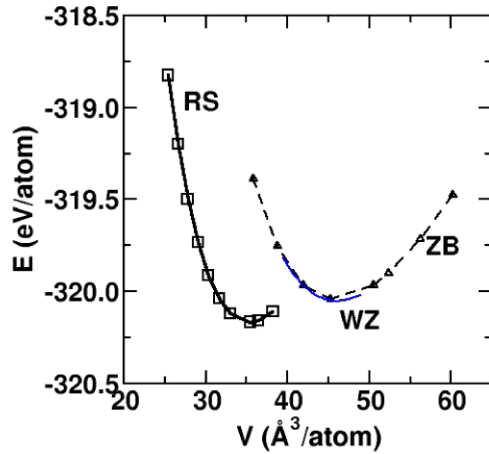


**Figure 1.** Energies of ZB, WZ and RS structures as a function of volume.

a tetragonal  $I\bar{4}m2$  and orthorhombic ( $Imm2$ ) intermediate state [8–10]. Such a tetragonal modification also formed in the classical MD simulation [1] but it was questioned in a first-principles calculation [6].

The magnesium chalcogenide, MgS, is a wide gap semiconductor and has a wide range of applications in optoelectronics [11] and luminescent devices [12]. MgS can crystallize in RS, ZB, and wurtzite (WZ) structures [13–17] but because of the small relative energy differences between the phases, its ground state and high pressure structure still remain a puzzle.

In this fast track communication, the constant pressure *ab initio* technique is performed to understand not only the behavior of ZB–MgS under pressure but also the sequence of high pressure structures for the  $A^N B^{N-8}$  compounds in general. We can consider the entire sequence because all  $A^N B^{N-8}$  materials, having an average of four valence electrons per atom, show some similarities in the structures that they adopt both under normal conditions and under applied pressure. The present simulation suggests that ZB–MgS transforms into a RS structure at high pressure. Unexpectedly it is found that the ZB-to-RS phase transformation proceeds by the  $R3m$  and  $R\bar{3}m$  intermediate phases. This transformation mechanism does not involve any bond breaking and it is different from the known mechanism based on  $I\bar{4}m2$  and  $Imm2$  intermediate states.

All calculations were performed using the SIESTA code [18], which is based on the first-principles pseudopotential method within the density functional theory. For the Kohn–Sham Hamiltonian, the generalized-gradient approximation (GGA) for the exchange correlation functional of Perdew, Burke and Ernzerhof [19] was chosen with norm conserving pseudopotentials of Troullier–Martin type [20]. A double-zeta plus polarization numerical basis set was selected together with a real-space mesh cutoff corresponding to an upper energy cutoff 200.0 Ryd. The simulation cell consists of 64 atoms with periodic boundary conditions.  $\Gamma$ -point sampling for the Brillouin zone integration was used for the simulation cell. The MD simulation was performed using the NPH (constant number of atoms, constant pressure, and constant enthalpy) ensemble.

**Table 1.** Equilibrium lattice parameters, the bulk modulus and its pressure derivative of the ZB, WZ and RS structures of MgS. References [28, 30] and [31] are experimental data.

Structure	$a$ (Å)	$c$ (Å)	$B_0$ (GPa)	$B'_0$	Reference
ZB	5.68		63	3.74	This study
	5.64		60	4.06	[24]
	5.61		60	3.89	[25]
	5.61		61	4.06	[26]
	5.46		71	4.16	
	5.66				[28]
WZ	4.042	6.508	63	3.47	This study
	3.996	6.492	63	4.18	[24]
	3.945	6.443	57	4.10	[29]
	3.969	6.487	64	2.96	[25]
	3.972	6.443			[30]
RS	5.29		89	3.99	This study
	5.18		81	4.15	[24]
	5.14		92	4.44	[25]
	5.14		82	3.98	[26]
	5.16		81	4.03	[27]
	5.19				[31]

ble. The reason for choosing this ensemble is to remove the thermal fluctuation, which facilitates easier examination of the structure during the phase transformation. Pressure was applied via the method of Parrinello and Rahman [21]. The equilibration period is 1000 time steps with a time step of 1 fs. The power quenching technique was also used during the MD simulations. In this technique, each velocity component is quenched individually. At each time step, if the force and velocity components have opposite signs, the velocity component is set equal to zero. All atoms or supercell velocities (for cell shape optimizations) are then allowed to accelerate at the next time step. For the energy–volume calculations, the unit cell of the ZB, WZ, and RS phases was considered. The Brillouin zone integration was performed with an automatically generated  $10 \times 10 \times 10$   $k$ -point mesh for both phases following the convention of Monkhorst and Pack [22].

The symmetry of phases was determined using the KPLOTT program [23] that provides detailed information about the space group, cell parameters and atomic position of a given structure. For the symmetry analysis 0.2 Å, 2°, and 0.7 Å tolerances for bond lengths, bond angles and interplanar spacing, respectively, were used.

In order to validate the parameters used in the simulations, the lattice constants of the ZB, WZ, and RS phases are first optimized and then compared with available experimental and theoretical data in table 1. Overall, the present results are in good agreement with experimental and theoretical values [24–31].

In order to predict the relative stability of the ZB, WZ, and RS phases, their energy–volume data are calculated and fitted to the third order Birch–Murnaghan equation of state. Figure 1 shows the computed total energy as a function of volume. Accordingly, the RS phase has the lowest energy and hence is the energetically more favorable one, in agreement with the previous DFT calculations [24]. The relative energy difference between the ZB and WZ phase is rather small. Such a small energy difference between these phases is anticipated because both structures have similar tetrahedral bonds.

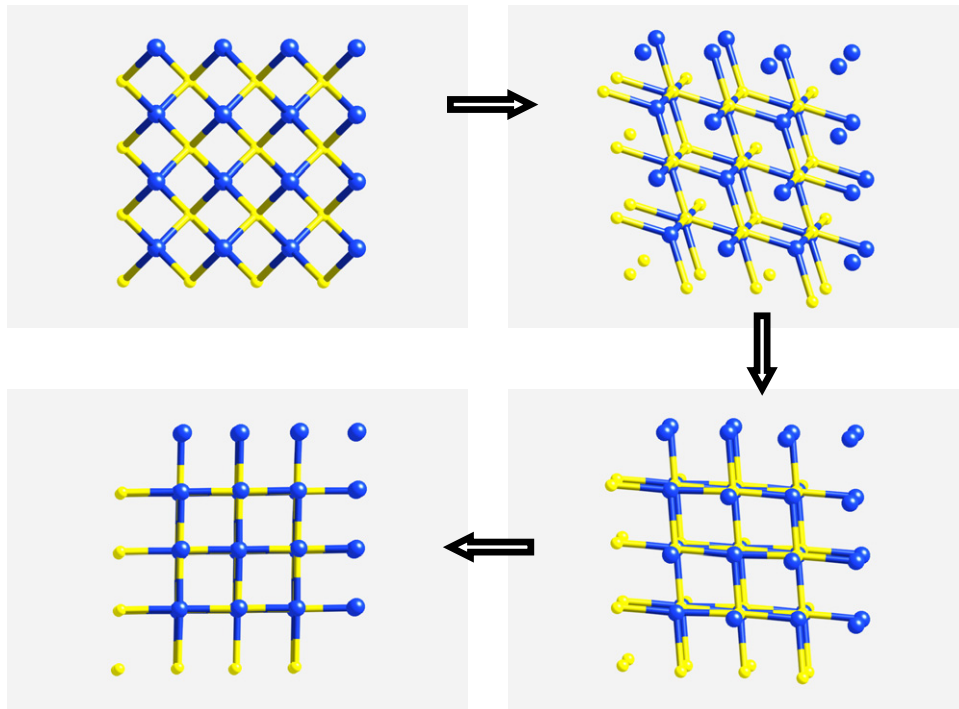


Figure 2. Evolution of the rocksalt structure at 75 GPa.

In the present MD simulations, the ZB structure is found to remain essentially intact until 60 GPa. As the pressure is increased from 60 to 75 GPa, the structural phase transition begins and is accompanied by a dramatic change in the simulation cell vectors. Owing to the transformation, the ZB structure converts into the RS structure as seen in figure 2.

Since the modification of the simulation box provides a clear picture about the transformation mechanism at the atomistic level, the change of the simulation cell lengths and angles at 75 GPa are carefully analyzed and plotted as a function of MD time steps in figure 3. The simulation cell vectors **A**, **B**, and **C** are initially along the [100], [010] and [001] directions, respectively. The magnitudes of these vectors are plotted in the figure. As one can see from the figure, the phase transformation is associated with shear deformation as indicated by the dramatic changes in the simulation cell angles. All the angles first gradually increase with the same magnitude up to 100 MD steps and then all angles decrease progressively to 90°. All simulation cell lengths have a tendency to decrease during the phase transformation but the decrease after 100 MD steps is more dramatic. The mechanism observed in the present simulation differs from the one (an initial tetragonal distortion and a successive shearing) obtained in other MD simulations. To our knowledge this mechanism has not been observed or proposed so far.

In order to determine the intermediate phase formed during the phase transformation, the structure at each MD step is carefully analyzed using the KLPOT program. During the simulation cell angles' increase, the formation of a  $R\bar{3}m$  (No:160) phase is observed. The  $\alpha$ ,  $\beta$  and  $\gamma$  angles ( $\alpha = \beta = \gamma$ ) of the  $R\bar{3}m$  phase gradually increase to about 75°. This phase is initially fourfold coordinated and the bond lengths have the same value. When the angles reach about 70°, this

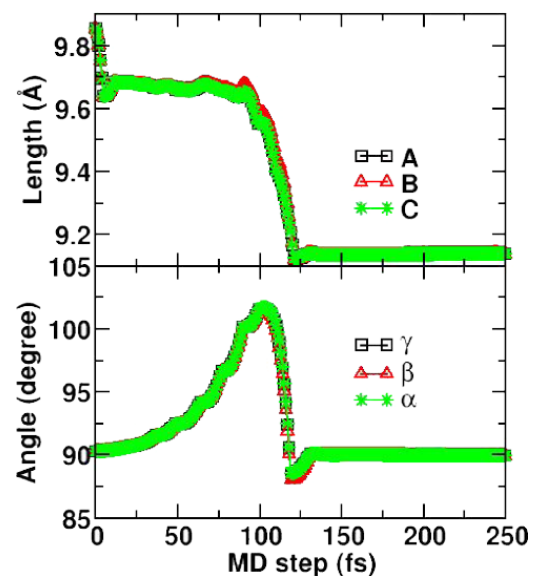


Figure 3. Change in the simulation cell lengths and angles as a function of MD time steps at 75 GPa.

phase can be considered as a very distorted sixfold coordinated structure (two new neighbor separations are slightly larger than the other four neighbor separations). During the simulation cell's decrease a  $R\bar{3}m$  (No: 166) phase is formed and its  $\alpha$ ,  $\beta$  and  $\gamma$  angles ( $\alpha = \beta = \gamma$ ) decrease monotonically to 60° at which point a RS structure is formed. The  $R\bar{3}m$  phase is sixfold coordinated and the angles among first neighbor atoms deviate from 90°. The evaluation of the RS phase is presented in figure 2. As can be seen from the figure, this phase transformation does not involve any bond breaking.

The symmetry analysis suggests that the ZB-to-RS phase transition is associated with two intermediate phases;  $R3m$  and  $R\bar{3}m$  phases. This mechanism is different from the previously proposed mechanism based on tetragonal  $I\bar{4}m2$  and orthorhombic  $Imm2$  intermediate states. One might think that the new mechanism observed for MgS is related to some limitations of the simulations such as the small size of the simulation box, loading conditions, etc. It should be noted here that using the same simulation technique, the size of the simulation box and loading condition, we observed the tetragonal  $I\bar{4}m2$  and orthorhombic  $Imm2$  intermediate states in SiC [8], ZnS [9] and ZnSe [10]. Consequently, these two dissimilar observations in these materials under similar simulation conditions suggest that the ZB-to-RS phase change might be material dependent. Currently it is unclear which properties of MgS produce this new transformation mechanism but its high ionicity is probably responsible for this new transformation path.

In conclusion, an *ab initio* constant pressure technique is applied to study the pressure-induced phase transition in the ZB-structured MgS. A phase transformation from the ZB crystal to a RS crystal is predicted through the simulation. The phase transformation proceeds via two intermediate phases with  $R3m$  (No:160) and  $R\bar{3}m$  (No:166) symmetries and does not involve any bond breaking. This mechanism is, for the first time, observed for the ZB-to-RS phase transformation and is most likely due to the ionicity of this material. The present study brings a new level of understanding to this phase transition.

The visit of the author to Ahi Evran Üniversitesi was facilitated by the Scientific and Technical Research Council of Turkey (TÜBİTAK) BİDEB-2221. The calculations were run on Sacagawea, the 128 processor Beowulf cluster, at the University of Texas at El Paso.

## References

- [1] Shimojo F, Ebbsjö I, Kalia R, Nakano A, Rino J P and Vashista P 2004 *Phys. Rev. Lett.* **84** 3338
- [2] Karch K, Bechstedt F, Pavone P and Strauch D 1996 *Phys. Rev. B* **53** 13400
- [3] Catti M 2000 *Phys. Rev. Lett.* **87** 35504
- [4] Perez-Mato J M, Aroyo M, Capillas C, Blaha P and Schwarz K 2003 *Phys. Rev. Lett.* **90** 49603
- [5] Miao M S and Lambrecht W R L 2005 *Phys. Rev. Lett.* **94** 225501
- [6] Miao M S and Lambrecht W R L 2002 *Phys. Rev. B* **66** 64107
- [7] Hatch D M, Stokes H T, Dong J, Gunter J, Wang H and Lewis J P 2005 *Phys. Rev. B* **71** 184109
- [8] Durandurdu M 2004 *J. Phys.: Condens. Matter* **16** 4411
- [9] Martinez I and Durandurdu M 2006 *J. Phys.: Condens. Matter* **18** 9483
- [10] Durandurdu M 2009 *J. Phys.: Condens. Matter* **21** 125403
- [11] Wang M W, Phillips M C, Swenberg J F, Yu E T, McCaldin J O and McGill T C 1993 *J. Appl. Phys.* **73** 4660
- [12] Pandey R and Sivaraman S J 1991 *Phys. Chem. Solids* **52** 211
- [13] Peiris S M, Campbell A J and Heinz D L 1994 *J. Phys. Chem. Solids* **55** 413
- [14] Okuyama H, Nakano K, Miyajima T and Akimato K 1992 *J. Cryst. Growth* **117** 139
- [15] Okuyama H, Nakano K, Miyajima T and Akimato K 1991 *Japan. J. Appl. Phys.* **30** L1620
- [16] Konczewicz L, Bigenwald P, Cloitre T, Chibane M, Ricou R, Testud P, Briot O and Aulombard R L 1996 *J. Cryst. Growth* **159** 117
- [17] Mittendorf H 1965 *Z. Phys.* **183** 113
- [18] Ordejón P, Artacho E and Soler J M 1996 *Phys. Rev. B* **53** 10441
- [19] Perdew J P, Burke K and Ernzerhof M 1996 *Phys. Rev. Lett.* **77** 3865
- [20] Troullier N and Martins J M 1991 *Phys. Rev. B* **43** 1993
- [21] Parrinello M and Rahman A 1980 *Phys. Rev. Lett.* **45** 1196
- [22] Monkhorst H J and Pack J D 1976 *Phys. Rev. B* **13** 5188
- [23] Hundt R, Schön J C, Hannemann A and Jansen M 1999 *J. Appl. Crystallogr.* **32** 413
- [24] Duman S, Bağcı S, Tütüncü H M and Srivastava G P 2006 *Phys. Rev. B* **73** 205201
- [25] Rached D, Benkhetto N, Soudini B, Abbar B, Sekkal N and Driz M 2003 *Phys. Status Solidi b* **240** 565
- [26] Drief F, Tadjer A, Mesri D and Aourag H 2004 *Catal. Today* **89** 11343
- [27] Kalpana G, Palanivel B, Thomas R M and Rajagopalan M 1996 *Physique B* **222** 223
- [28] Konczewicz L, Bigenwal P, Cloitre T, Chibane M, Ricou R, Testuo P, Briot O and Aulombard R L 1996 *J. Cryst. Growth* **159** 117
- [29] Lee S G and Chang K J 1995 *Phys. Rev. B* **52** 1918
- [30] Villars P and Calvert L D 1985 *Pearson's Handbook of Crystallographic Data for Intermetallic Phases* (Metals Park, OH: American Society of Metals)
- [31] Wyckoff R W G 1963 *Crystal Structures* (New York: Wiley)